Dielectric selective mirror for intracavity wavelength selection in far-infrared p-Ge lasers

T. W. Du Bosq, R. E. Peale, E. W. Nelson, A. V. Muravjov, C. J. Fredricksen, N. Tache, and D. B. Tanner

Articles you may be interested in

Neutron transmutation doped far-infrared p- Ge laser
J. Appl. Phys. **96**, 1 (2004); 10.1063/1.1753659

Single axial-mode selection in a far-infrared p-Ge laser
Appl. Phys. Lett. **76**, 1996 (2000); 10.1063/1.126233

Far-infrared laser oscillation from a very small p- Ge crystal under uniaxial stress
Appl. Phys. Lett. **74**, 3432 (1999); 10.1063/1.124118

Pulse separation control for mode-locked far-infrared p-Ge lasers
Appl. Phys. Lett. **74**, 167 (1999); 10.1063/1.124221

Gain of the mode locked p-Ge laser in the low field region
Appl. Phys. Lett. **72**, 1140 (1998); 10.1063/1.120995

Dielectric selective mirror for intracavity wavelength selection in far-infrared *p*-Ge lasers

T. W. Du Bosq, R. E. Peale,[a)] E. W. Nelson, and A. V. Muravjov[b)]
Department of Physics, University of Central Florida, Orlando, Florida 32816-2385

C. J. Fredricksen
Zaubertek, Inc., 12565 Research Parkway, Suite 300, Orlando, Florida 32826

N. Tache and D. B. Tanner
Department of Physics, University of Florida, Gainesville, Florida 32611-8440

A robust metal-free intracavity fixed-wavelength selector for the cryogenically cooled far-infrared *p*-Ge laser is demonstrated. The device is a back mirror consisting of a thin silicon etalon and dielectric $SrTiO_3$ flat. A laser line width of 0.2 cm^{-1} is achieved, which corresponds to an active cavity finesse of ~0.15. The wavelength position and spectral purity are maintained over a wide range of laser operating fields. Use of $SrTiO_3$ lowers the laser resonance line frequencies by ~1 cm^{-1} compared with expectations for metal mirrors. The effect is due to phase shift, which is determined from far-infrared reflectivity measurements of $SrTiO_3$. A *p*-Ge laser with such selector is free from danger of electrical breakdown and mirror oxidation during repeatable thermal cycling, which makes it more reliable than previous selection schemes for practical applications. © *2003 American Institute of Physics.* [DOI: 10.1063/1.1618934]

INTRODUCTION

Recent developments of semiconductor lasers in the terahertz range of the electromagnetic spectrum include intra-valence-band *p*-Ge lasers,[1] Si lasers based on optically pumped donors,[2] and quantum cascade lasers (QCLs).[3–5] Their availability is stimulating development of new applications in chemical sensing, THz imaging, and nondestructive testing. Most such applications require spectral purity and stability of the laser line. The *p*-Ge laser differs from Si lasers and QCL by having a very broad gain bandwidth (1.5–4.2 THz). While this permits wide tunability, it prevents generation of a spectrally pure line without operating in cyclotron resonance mode[6] or the use of special means of electrodynamic mode selection.[7–9]

The *p*-Ge laser emission spectrum can be 20–30 cm^{-1} wide. For a typical laser cavity of several centimeters length, such a spectrum contains hundreds of longitudinal modes. Cyclotron resonance operation or external spectral selection both substantially reduce output power. In contrast, a *p*-Ge laser with practical intracavity means of wavelength selection would maintain peak output power at the level of watts, which certain applications may require.

Selective cavities have been demonstrated[7–9] with active cavity finesse exceeding unity, resulting in single longitudinal mode emission.[10] The selector can be tuned *in situ* with piezoelectric control, allowing fine tuning between nearby longitudinal modes.[11] Recently, a variable-length cavity was demonstrated, which in principle allows continuous tuning without mode hops.[12] Nevertheless, the dream of a practical *p*-Ge laser with wavelength selection remains elusive after nearly two decades of research.

Difficulties in selector design include factors such as the cryogenic operating temperature, high operating voltages, and the high Ge refractive index. Past problems include fixed cavity length (allowing only discontinuous tuning between fixed longitudinal modes), planar metal mirrors (that tarnish, scratch, require dielectric isolation, and cause high alignment sensitivity), intracavity interfaces (introducing unwanted intrinsic resonances, parasitic scattering, and reflections[11,13]), and moving parts (that stick when cooled). Additionally, at cryogenic temperatures, piezocontrol gives only small displacements, even at high control voltages, resulting in a limited tuning range.[11] Clearly, new selector concepts are required for the *p*-Ge laser.

In this article, a wavelength selective back mirror formed completely of dielectric components is considered. This design is a modification of the well-known method of laser wavelength selection using intracavity etalons.[14,15] It consists of a combination of Si etalon and $SrTiO_3$ flat[16] (Fig. 1). Selection with etalons is generally advantageous in practical applications that require stable, repeatable, laser line frequencies, such as sensing of specific chemical compounds. Advantages of the present design for *p*-Ge lasers is the absence of any metallic components, eliminating the requirement of insulating films or spacers between the electrically excited active crystal and other cavity elements. This feature minimizes the number of required intracavity interfaces, eliminating all unwanted intrinsic resonances. Nonmetallic mirrors are also more stable against scratching and tarnishing. This dielectric design permits use of very thin
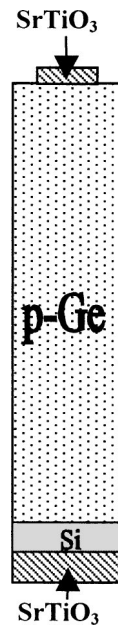
FIG. 1. Construction of p-Ge laser intracavity etalon wavelength selector.

etalons, operating on low (1,2,3) resonance orders, without danger of electrical breakdown.

Wavelength selection in p-Ge lasers using an intracavity etalon has been reported previously[17] although this cavity was complicated by multiple intracavity interfaces and curved mirror surfaces. The reported emission line width was $\sim$1 cm^{-1} with additional parasitic resonances separated from the main line by $\sim$1.1 cm^{-1} on top of a broad background. In contrast, the present work achieves an emission line width of 0.2 cm^{-1} with no background or additional features.

EXPERIMENTAL DETAILS

Thin, two-side-polished, silicon wafers were obtained from Valley Design. Wafers were specified flat and parallel within 4 arc-secs, which exceeds the usual 30-arc-sec requirements for p-Ge laser plane-mirror-cavity constructions. Room-temperature measurement of interference fringes in the range 4900 to 5100 cm^{-1} gave values for thickness of 95.9$\pm$1.2 (etalon A) and 113.6$\pm$0.7 μm (etalon B). These values depend on the room-temperature silicon refractive index at 2 μm wavelength, for which the value 3.453$\pm$0.002 was used.[18] Near-IR etalon spectra were obtained using a

Fourier spectrometer with quartz beamsplitter and InSb detector. The stated uncertainty in wafer thickness is due primarily to experimental uncertainty in the average fringe spacing, which defines the etalon fundamental at 2 μm wavelength and 300 K. The fractional change in wafer thickness is estimated to be only $\sim$10^{-5} on cooling to 4 K and can be ignored.

To determine the etalon fundamental ν_0 near 100 μm wavelength and 4 K temperature, the relation

$$\nu_0 = (n'_{Si}/n_{Si}) \nu'_0 \tag{1}$$

was used, where the prime refers to 2-μm and 300-K values. The index n_{Si} of silicon at 100 μm wavelengths and 4 K temperature[19] is 3.384$\pm$0.002. The etalon fundamental values found from Eq. (1) are listed in Table I along with the etalon thickness values.

The laser crystal was cut from p-type germanium purchased from Tydex (St. Petersburg, Russia). The rectangular rod had dimensions 45.7 mm$\times$7 mm$\times$5 mm. The axial direction was parallel to [110]. The longer transverse direction was parallel to [1$\bar{1}$0] and the shortest was parallel to [001]. End faces were polished flat and parallel within 30 arc-sec. Indium ohmic contacts were applied to opposite lateral faces with an ultrasonic soldering iron so that electric-field pulses could be applied in the [1$\bar{1}$0] orientation with a thyratron pulser. The laser cavity was constructed by sandwiching the active crystal and thin silicon spacer between two polished SrTiO$_3$ mirrors (Fig. 1). The aperture of one of the mirrors was smaller than the active crystal end face for output coupling. The resulting longitudinal mode spacing for the entire cavity is about 0.028 cm^{-1}. A magnetic field was applied using a superconducting solenoid attached to a light pipe insert for liquid-helium storage dewars. The laser was operated at repetition rates of 1–8 Hz and with pulse duration 1 μs.

Spectroscopy of laser emission was performed on a Bomem DA8 vacuum-bench Fourier spectrometer using an event-locking[20] accessory (Zaubertek) at resolutions up to 0.04 cm^{-1}. Frequency accuracy has been verified by comparing argon laser lines measured with the accessory and by the Bomem standard method.[20] A Mylar™ pellicle beamsplitter and a 4-K silicon composite bolometer (Infrared Labs) were used. Peak far-infrared power and beam divergence at the output of the light pipe were estimated to be 1 W and 26°, respectively, using a room temperature golay cell (QMC In-

TABLE I. Experimental and theoretical parameters related to intracavity silicon etalons. The discrepancy is the fractional difference between the predicted resonance and the nearest observed laser line.

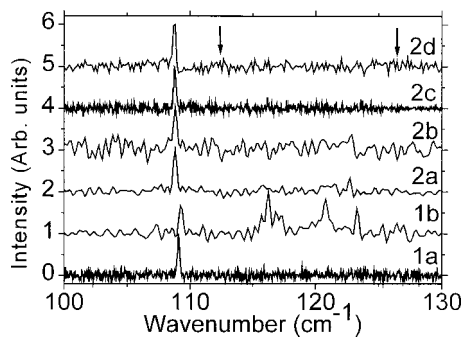|	Etalon A		Etalon B	
Etalon thickness d (μm)	95.9$\pm$1.2		113.6$\pm$0.7	
Etalon fundamental ν_0 (cm^{-1})	14.17$\pm$0.17		12.74$\pm$0.08	
$\nu_9 - \nu_8$ (cm^{-1})	14.2$\pm$0.3		11.3$\pm$0.5	
Resonance order m	8	9	8	9
Phase shift (rad)	0.43	0.51	0.38	0.42
Predicted line ν_m (cm^{-1})	112.4$\pm$1.4	126.4$\pm$1.5	101.1$\pm$0.6	113.8$\pm$0.7
Observed line (cm^{-1})	109.1$\pm$0.1	123.3$\pm$0.3	94.8$\pm$0.5	106.1$\pm$0.5
Percent discrepancy (%)	3	2.5	6	7

FIG. 2. Emission spectra of far-infrared *p*-Ge laser with 95.9 μm silicon intracavity etalon. Spectra 1a and 2c were collected at 0.1 cm^{-1} resolution. The other spectra were collected at 0.5 cm^{-1} resolution. Arrows indicate predicted positions of selector resonances.

FIG. 4. Expanded spectrum 1a with 95.9 μm silicon intracavity etalon at 0.1 cm^{-1} resolution. The laser line has a full width at half-maximum of 0.2 cm^{-1}.

struments). The laser was strongly attenuated at the spectrometer input using a partial beam block to avoid saturating the bolometer.

The reflectance of SrTiO$_3$ was measured over the range 0 to 5000 cm^{-1} using a Bruker 113v. Fourier spectrometer in conjunction with an Infrared Laboratories 4.2-K Si bolometer. The sample was located in vacuum, at the tip of a Hanson continuous-flow cryostat, providing temperatures between 20 and 300 K. The phase shift on reflection was estimated using Kramers–Kronig analysis. The reflectance was extrapolated as ν^{-1} from 5000 to 10^5 cm^{-1} and as ν^{-4} at higher frequencies. It was extended to zero frequency using the parameters of a fit using multiple Lorentz oscillators. The real and imaginary parts of the complex index of refraction (n_{srt} and κ_{srt}, respectively) were determined from the reflectance and phase shift by inverting the Fresnel relations.

In the laser experiments, the far-infrared beam is incident on the SrTiO$_3$ from crystalline silicon (Fig. 1). In this case, the phase shift is determined from the real index of silicon n_{Si} at 100 μm wavelength and 4 K temperature, and from the real and imaginary parts of the SrTiO$_3$ index according to

$$\tan \phi = 2 \kappa_{srt} n_{Si} / (n_{srt}^2 + \kappa_{srt}^2 - n_{Si}^2). \qquad (2)$$

The effect of incidence from silicon is to increase the phase shift by roughly a factor n_{Si} over the value found for vacuum incidence.
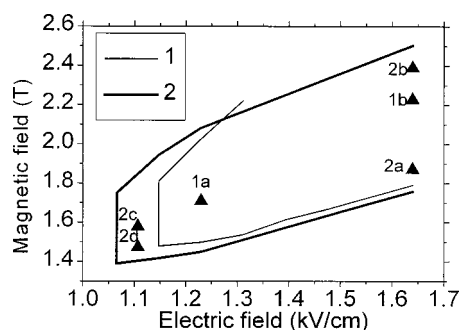
RESULTS

Figure 2 presents laser emission spectra at resolution of 0.1 or 0.5 cm^{-1} using etalon A for different applied fields (Fig. 3). Except for spectrum 1b, the spectra are characterized by a single line at 109.1 cm^{-1}. The position of this line is not affected by the thermal cycling and cavity reassembly. In spectrum 1b, however, the line shifts slightly to higher frequency, and additional lines appear at 116.3, 120.8, and 123.3 cm^{-1}. Figure 4 is an expanded version of spectrum 1a to show that the full width at half-maximum is 0.2 cm^{-1}.

Figure 5 presents a laser emission spectrum taken with etalon B. Two lines are observed at 94.8 and 106.1 cm^{-1}. Figure 5 is an average of two spectra taken at 1 cm^{-1} resolution. Increased noise for the Fig. 5 spectrum (compared with Fig. 2) limited practical resolution to 1 cm^{-1}. The explanation is shot-to-shot spectral instability in the two-line operation mode, which is missing in the single-line mode (Fig. 2).

Figures 6 and 7 show respective plots of the reflectance of SrTiO$_3$ and the phase shift, for incidence from vacuum and sample temperatures of 20 and 50 K. The plot range is limited to the tuning range for Ga-doped Ge laser crystals. Long and short period oscillations are artifacts that cause the reflectance to exceed unity at frequencies near 100 cm^{-1}. The maximum value of reflectance in the data file is 1.0060. Errors are 1% (a 2σ value) in random noise and about 1% in systematic error. The Kramers–Kronig routine clips the data to 1.0 when it exceeds this value to stay in the physical

FIG. 3. Laser generation zones for different spectroscopic experiments. Symbols indicate *E* and *B* values for spectra presented in Fig. 2. In between the measurements corresponding to the two threshold curves, the laser was warmed to room temperature and the cavity was completely reassembled.
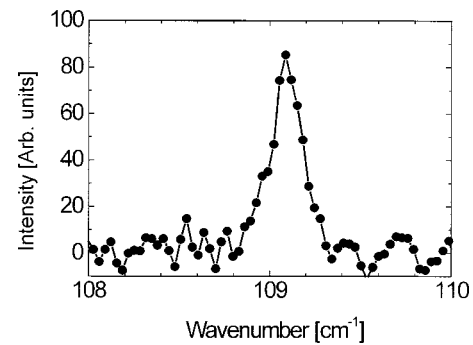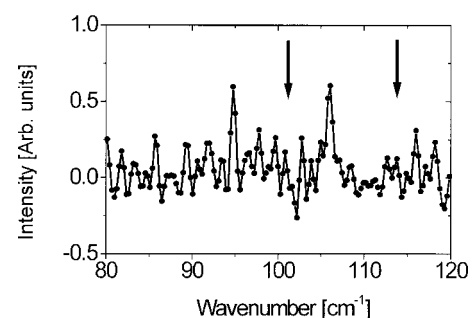

FIG. 5. Emission spectrum with 113.6 μm silicon intracavity etalon at 1 cm^{-1} resolution. Arrows indicate predicted positions of etalon resonances.
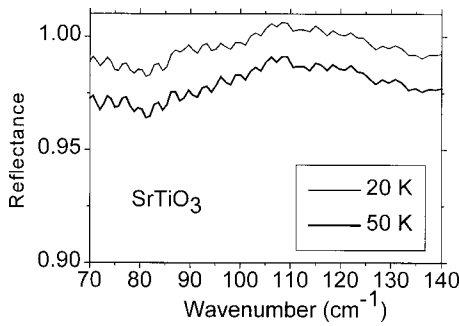
FIG. 6. Reflectance of SrTiO$_3$ in the tuning range of the Ga-doped *p*-Ge laser.
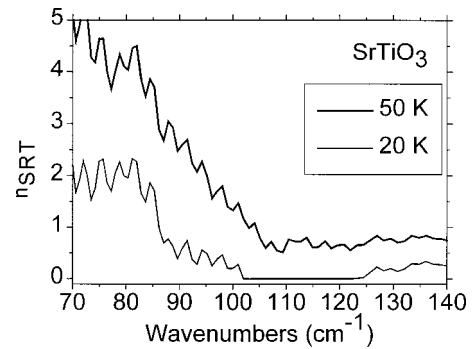

FIG. 8. Real part of the SrTiO$_3$ index of refraction.

regime. This procedure keeps the phase shift in the right quadrant and the real part of the index positive. Phase uncertainty is estimated to be about 10%.

Figures 8 and 9 are respective plots of n_{srt} and κ_{srt} for SrTiO$_3$ at temperatures of 50 and 20 K. Values for the phase determined from these data using Eq. (2) for incidence from Si are given at each observed laser wavelength in Table I.

DISCUSSION

Figure 3 reveals the degree to which the laser generation zone of E and B fields applied to the active crystal may vary as a result of thermal cycling and reconstruction of the cavity. The zone can also depend on the magnetic-field polarity and on uncontrollable factors related to assembly of the laser cavity, including changes in mirror position, cleaning of optical surfaces, quality of the contacts, quality of the germanium, and placement within the solenoid. A reliable wavelength selector, therefore, should be designed to be independent (as far as possible) of the applied fields. A positive result of this work is that a single narrow emission line can be produced at a stable wavelength over a wide range of fields. Indeed, it was difficult to find fields within the generation zone where the laser operated exclusively on a different spacer resonance.

A laser line width of ~ 0.2 cm^{-1} was found from spectra taken at 0.1 cm^{-1} resolution, as shown in Fig. 4. Absence of structure within the line profile was confirmed by a spectrum taken at 0.04 cm^{-1} resolution. The achieved line width is five times narrower than previously reported using intracavity etalon selection for a *p*-Ge laser, and side lobes or broad

background are absent.[17] The emission line consists of about seven longitudinal modes, giving an active cavity finesse of ~ 0.15.

Table I gives expected resonance values, which are calculated according to

$$\nu_m = \nu_0 (m - \phi/2\pi), \tag{3}$$

where m is an integer, ϕ is the phase shift on reflection from SrTiO$_3$ (Table I), and ν_0 is the etalon fundamental at 100 μm wavelength and 4 K temperature (Table I). A positive phase shift is equivalent to reflection from a layer below the SrTiO$_3$ surface. Therefore, the effect of the phase shift is to decrease the laser line frequency. Given the ϕ and ν_0 values in Table I, this shift is about 1 cm^{-1}.

The expected laser line positions ν_8 and ν_9 (Table I) are indicated in Figs. 2 and 5 by arrows. Table I gives the percent discrepancy between predicted and observed line positions. The discrepancy is about twice the estimated uncertainties. One might consider a possible air gap between active crystal and etalon, or between etalon and SrTiO$_3$ back mirror, as increasing the effective thickness of the etalon and thus lowering actual laser line positions relative to predicted values. However, the number (2 or less) and symmetry (circular) of Newton's rings seen through the SrTiO$_3$ mirror during cavity assembly, the etalon flatness specification, typical laser-rod end flatness, and the <30-arc-sec allowable antiparallelness for lasing, all limit the likely air gap to less than 1 μm. The possibility of such a gap effectively doubles the percent uncertainty in predicted laser line position, which would be just enough to explain the discrepancy for etalon A. Although ability to predict the position of *p*-Ge laser lines
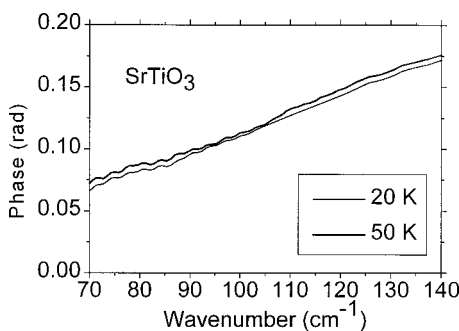

FIG. 7. Phase shift on reflection from SrTiO$_3$ with incidence from vacuum.
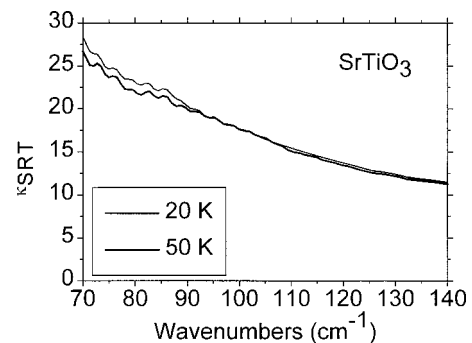

FIG. 9. Imaginary part of the SrTiO$_3$ index of refraction.

using a silicon etalon selector is apparently not yet better than several percent, results presented here suggest that measured values will be at least repeatable to within about 0.1 cm^{-1} for different cavity assemblies using the same etalon.

Note that in Fig. 5, the arrow for ν_8 falls about midway between the observed lines. Hence, the observed lines could have been attributed to the seventh and eighth etalon resonances with equivalent discrepancies. Despite this uncertainty in assignment, the separation between observed lines, also given in Table I, is the nearly the same (for both Fig. 5 and Fig. 2 data) within estimated uncertainty as the etalon fundamental, and confirms its role in the selection.

Figure 2 spectrum 1b contains two additional unexpected lines that are apparently unrelated to etalon resonances. These lines might arise from amplification on harmonics of light-hole cyclotron resonance, since the magnetic field here is already quite strong. If the gain is sufficiently high, as expected near the zone center, such resonances can be pronounced despite the presence of the wavelength selector in the cavity. In addition the main line at ~109 cm^{-1} seems slightly shifted with respect to the other spectra, although the shift is less than the 0.5 cm^{-1} resolution of this spectrum. When the gain is above the absorption level over an extended spectral range, the line position might be influenced by some other resonance features of the cavity or gain. By moving away from zone center, which lowers the gain, the etalon resonance again dominates, and single-line emission is restored.

CONCLUSIONS

A simple metal-free design of a fixed-wavelength intracavity selector for the far-infrared *p*-Ge laser has been demonstrated. Use of only dielectric components eliminates need for insulating films or spacers in the cavity, which were previously necessary[7,8,10,11,17] to prevent electrical breakdown, but which caused parasitic reflections and worsened the spectral purity of the laser line. Although in this article we demonstrated selection using fairly thick etalons operating on ~ eighth order of resonance, this design allows use of very thin etalons that operate on the lower resonance orders without danger of breakdown.

The emission wavelength was found to be stable over a wide range of operating electric and magnetic fields and is unaffected by thermal cycling or reconstruction of the laser cavity. At high fields, when the laser gain is high, additional lines appear, but such field regions are easily avoided. The narrowest laser line width observed was 0.2 cm^{-1}. This line consists of about seven longitudinal modes, giving an active

cavity finesse of 0.15. Phase shift from reflection on the SrTiO$_3$ back mirror, which was used in conjunction with the etalon, lowers *p*-Ge laser line positions by only about 1 cm^{-1} (relative to positions obtained using a metal back mirror). However, for the larger fundamentals of thinner etalons, the shift in wave numbers caused by phase shift would be proportionally larger. A *p*-Ge laser equipped with an etalon selector easily can be prepared to operate in regions of relatively high atmospheric transmission for applications in chemical sensing, THz imaging, and nondestructive testing.

[1] Special issue of Opt. Quantum Electron. **23**, S111-S322 (1991), edited by E. Gornik and A. A. Andronov.

[2] S. G. Pavlov, Kh. Zhukavin, E. E. Orlova, V. N. Shastin, A. V. Kirsanov, H.-W. Huebers, K. Auien, and H. Riemann, Phys. Rev. Lett. **84**, 5220 (2000).

[3] B. S. Williams, H. Callebaut, S. Kumar, Q. Hu, and J. L. Reno, Appl. Phys. Lett. **82**, 1015 (2003).

[4] R. Köhler, A. Tredicucci, F. Beltram, H. E. Beere, E. H. Linfield, A. G. Davies, D. A. Ritchie, R. C. Iotti, and F. Rossi, Nature (London) **417**, 156 (2002).

[5] M. Rochat, L. Ajili, H. Willenberg, J. Faist, H. Beere, G. Davies, E. Linfield, and D. Ritchie, Appl. Phys. Lett. **81**, 1381 (2002).

[6] E. Gornik, K. Unterrainer, and C. Kremser, Opt. Quantum Electron. **23**, S267 (1991).

[7] A. V. Murav'ev, I. M. Nefedov, S. G. Pavlov, and V. N. Shastin, Quantum Electron. **23**, 119 (1993).

[8] S. Komiyama, H. Morita, and I. Hosako, Jpn. J. Appl. Phys. **32**, 4987 (1993).

[9] A. A. Andronov, V. A. Kozlov, S. A. Pavlov, and S. G. Pavlov, Opt. Quantum Electron. **23**, S205 (1991).

[10] A. V. Muravjov, S. H. Withers, H. Weidner, R. C. Strijbos, S. G. Pavlov, V. N. Shastin, and R. E. Peale, Appl. Phys. Lett. **76**, 1996 (2000).

[11] E. W. Nelson, A. V. Muravjov, S. G. Pavlov, V. N. Shastin, and R. E. Peale, Infrared Phys. Technol. **42**, 107 (2001).

[12] A. V. Muravjov, E. W. Nelson, R. E. Peale, V. N. Shastin, and C. J. Fredricksen, Infrared Phys. Technol. **44**, 75 (2003).

[13] E. W. Nelson, S. H. Withers, A. V. Muravjov, R. C. Strijbos, R. E. Peale, S. G. Pavlov, V. N. Shastin, and C. J. Fredricksen, IEEE J. Quantum Electron. **12**, 1525 (2001).

[14] P. W. Smith, Proc. IEEE **60**, 422 (1972).

[15] A. E. Siegman, *Lasers* (University Science, Mill Valley, CA, 1986), pp. 524–531.

[16] A. V. Bespalov, P. T. Lang, J. Betz, and K. F. Renk, Appl. Phys. Lett. **58**, 2030 (1991).

[17] K. Unterrainer, M. Nithisoontorn, M. Helm, E. Gornik, and E. E. Haller, Infrared Phys. **29**, 357 (1989).

[18] C. D. Salzberg and J. J. Villa, J. Opt. Soc. Am. **47**, 244 (1957).

[19] E. V. Loewenstein, D. R. Smith, and R. L. Morgan, Appl. Opt. **12**, 398 (1973).

[20] H. Weidner and R. E. Peale, Appl. Spectrosc. **51**, 1106 (1997).